Improving SAR Images: Built-In Geometric and Multi-Look Radiometric Corrections

O. O. Bezvesilniy, Ie. M. Gorovyi, S. V. Sosnytskiy, V. V. Vynogradov, D. M. Vavriv

Department of Microwave Electronics, Institute of Radio Astronomy of NAS of Ukraine
4 Chervonopraporna Str., Kharkov 61002, Ukraine
`obezv@rian.kharkov.ua`

Abstract—**SAR systems installed on small aircrafts and UAVs suffer from trajectory deviations and instabilities of antenna orientation. These kinds of motion errors lead to significant geometric distortions and radiometric errors in SAR images. In the paper, we describe a time-domain multi-look stripmap SAR processing algorithm with built-in geometric and multi-look radiometric corrections. Geometric correction is performed due to azimuth reference functions and range migration curves specially designed to produce SAR images directly on a rectangular grid on the ground plane. Radiometric correction is based on multi-look processing with extended number of looks. The proposed techniques have been successfully tested with a Ku-band SAR system installed on a light-weight aircraft.**

I. INTRODUCTION

The formation of high-quality multi-look SAR images with SAR systems installed on small aircrafts or UAVs is a difficult problem because of significant motion and orientation errors of such light-weight platforms. Deviations of the aircraft trajectory and instabilities of the antenna orientation lead to geometric and radiometric errors in SAR images [1]-[3].

Geometric distortions in SAR images can be corrected by interpolation of images to a rectangular grid on the ground plane taking into account the measured aircraft trajectory and the orientation of the synthetic aperture beams. However, this approach becomes inefficient in case of significant geometric distortions.

The clutter lock technique is usually used to avoid radiometric errors in SAR images [1], [4]. According to this technique, the azimuth reference functions are built adaptively to track time variations of the Doppler centroid. It means that all SAR look beams are kept within the real antenna beam and the central SAR look beam is pointed exactly at the center of the real antenna beam. However, the clutter-lock should not be used in case of fast and significant instabilities of the antenna orientation when it leads to strong geometric errors in SAR images.

Instabilities of the aircraft orientation can be compensated by the antenna stabilization. It is a complicated and expensive solution. The application of a wide-beam antenna firmly mounted on the aircraft is another way to guarantee the uniform illumination of the ground scene despite of the instabilities of the platform orientation. This is a good solution; however it requires the operation at higher pulse repetition frequency.

In this paper, we propose a time-domain multi-look stripmap SAR processing algorithm with built-in correction of geometric distortions. The azimuth reference functions and range migration curves are specially designed to produce SAR images directly on a rectangular grid on the ground plane. In this way, we immediately obtain geometrically correct SAR images.

This approach cannot be combined with the clutter-lock and radiometric errors could appear in case of fast and considerable instabilities of the antenna orientation, especially for narrow-beam antenna. To solve this problem, we have proposed an effective radiometric correction technique based on multi-look processing with extended number of looks.

Both proposed techniques have been successfully tested by using a Ku-band airborne SAR system [5].

II. BUILT-IN GEOMETRIC CORRECTION

A. Time-Domain SAR Processing Algorithm

The proposed SAR processing algorithm is based on the one-dimensional time-domain convolution of the signals interpolated from range-compressed data along the migration curves

$$R_m(\tau) \approx R_m - (\lambda/2)F_{DC}(R_m)\tau - (\lambda/2)F_{DR}(R_m)\tau^2/2 \quad (1)$$

with the reference functions

$$h_m(\tau) = w_m(\tau)\exp[i(4\pi/\lambda)R_m(\tau)]. \quad (2)$$

Here R_m is the slant range, m is the range cell index, λ is the radar wavelength, $w_m(\tau)$ are the weighting windows applied for the side-lobe control.

The Doppler centroid F_{DC} and the Doppler rate F_{DR} are given by

$$F_{DC}(R_m) = \frac{2}{\lambda}\frac{(\vec{\mathbf{R}}_m \cdot \vec{\mathbf{V}})}{R_m}, \quad (3)$$

$$F_{DR}(R_m) = -\frac{2}{\lambda}\left[\frac{V^2}{R_m}\left(1 - \frac{(\vec{\mathbf{R}}_m \cdot \vec{\mathbf{V}})^2}{R_m^2 V^2}\right) - \frac{(\vec{\mathbf{R}}_m \cdot \vec{\mathbf{A}})}{R_m}\right], \quad (4)$$

where $\vec{\mathbf{V}}$ and $\vec{\mathbf{A}}$ is the aircraft velocity and the aircraft acceleration vectors, respectively.
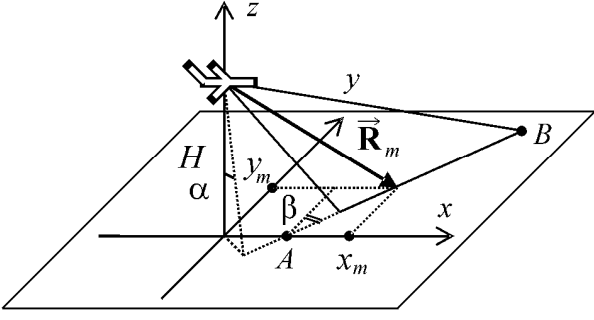
Fig. 1: Stripmap SAR geometry.

The slant range vector $\vec{\mathbf{R}}_m = (x_m, y_m, -H)$ goes from the antenna phase center to the point (x_m, y_m) on the ground at which the synthetic beam will be pointed (see Fig. 1), H is the aircraft flight altitude. The x-axis of the local coordinate system is pointed along the horizontal component of the aircraft velocity vector (so that $V_y = 0$). The z-axis is pointed upward and goes through the antenna phase center,. The point (x_m, y_m) is on the Doppler centroid line AB which is the intersection of the elevation plane of the real antenna pattern and the ground plane. The orientation of the real antenna beam is described by the antenna pitch angle α and the antenna yaw angle β.

The described SAR algorithm is effective for building moderate-resolution SAR images when the convolution is not too long. The advantage of the algorithm is its ability to build each pixel of the SAR image with a particular reference function and migration curve taking into account time-varying and range-dependent Doppler centroid and Doppler rate.

B. Time-Domain Multi-Look Processing

The multi-look SAR processing is used to suppress speckle noise in SAR images [1], [6], as well as for other applications, for example for measuring the Doppler centroid with high accuracy and high spatial resolution [7], [8].

The time-domain multi-look processing is usually based on dividing the single reference function determined on the long coherent processing time interval $T_{S\max}$ on several reference functions determined on sub-intervals of synthetic aperture length T_S. The SAR look beams produced with these reference functions are pointed at the same point (x_m, y_m) on the ground. The difficulty with this approach is that we should guarantee that there are no significant uncompensated phase errors during the long coherent processing time $T_{S\max}$. However, in order to achieve the desired azimuth resolution, it is sufficient to process the phase coherently on the much shorter time interval T_S.

We use another approach to multi-look processing, which is more preferable in case of significant motion errors and for SAR processing with many looks (up to 100 in our experiments). We process the data collected during the time of

synthesis T_S with a set of different reference functions to form SAR look beams pointed at different points on the ground. These reference functions represent the half-overlapped sub-bands of the whole azimuth Doppler frequency band. The central frequencies and the width of the sub-bands are

$$F_{DC}(m,n) = F_{DC}(R_m) + n\Delta F_D / 2 , \qquad (5)$$

$$\Delta F_D = 2 F_{DR} T_{S\max} /(N_L + 1) , \qquad (6)$$

where $n = 0, \pm 1, ..., \pm N_L / 2$ is the SAR look index. Taking into account the relation for the azimuth resolution,

$$\rho_X = K_w V_X /(| F_{DR} | T_S) , \qquad (7)$$

(the coefficient K_w describes broadening of the main lobe of the synthetic aperture pattern caused by windowing) the central frequencies of the SAR looks (5) can be written as

$$F_{DC}(m,n) = F_{DC}(R_m) - n K_w V_X /(2\rho_X) . \qquad (8)$$

The SAR look beam formed with the central frequency (8) will be pointed to some point $(x_m + \xi_n, y_m + \eta_n)$. What are the coordinates of this point? First, since the signal from this point appears at the slant range R_m (at the center of the synthetic aperture) we can write:

$$x_m^2 + y_m^2 = (x_m + \xi_n)^2 + (y_m + \eta_n)^2 . \qquad (9)$$

Second, the position of the point in azimuth direction is related to its Doppler centroid (3) so that

$$F_{DC}(m,n) = F_{DC}(R_m) + (2/\lambda)V_X \xi_n / R . \qquad (10)$$

Thus, in order to form the set of SAR looks for slant range R_m with central frequencies (8) we should first calculate the corresponding points $(x_m + \xi_n, y_m + \eta_n)$ on the ground from (9) and (10) and then process the same raw data on the interval of synthesis T_S with the appropriate range migration curves (1), Doppler centroids (3) and Doppler rates (4).

Since the SAR look beams are aimed at different points on the ground, the SAR look images are appeared to be sampled on different grids. It means that SAR look images should be re-sampled to the same ground grid prior to averaging them into the multi-look image. The deviations of the aircraft trajectory introduce further complexity into the re-sampling process.

In this paper we propose a built-in geometric correction algorithm, in which the azimuth reference functions and range migration curves are specially designed to point SAR look beams directly at nodes of a rectangular grid on the ground plane, avoiding complicated re-sampling procedure.

C. Pointing SAR look beams at Nodes of a Rectangular Grid

The built-in geometric correction consists of the following steps. First, we should specify the reference flight trajectory with constant aircraft flight altitude, velocity, pulse repetition frequency, and antenna pitch and yaw angles. These reference

parameters are used to calculate the time-independent Doppler centroid $F_{DC}(R_m)$, the central Doppler frequencies of SAR looks $F_{DC}(m,n)$, and coordinates of the reference points on the ground plane at which the SAR look beams should be pointed $x_{ref}(n, R_m)$ and $y_{ref}(n, R_m)$. After that we should find the nodes of the rectangular grid on the ground which are close to these points (by using interpolation) $x_{ref}^{node}(n, i_Y)$, $y_{ref}^{node}(n, i_Y)$, i_Y is the ground range index of the grid.

Finally, we should point the synthetic beams to the corresponding nodes $x_{ref}^{node}(n, i_Y) + i_X \Delta x$, $y_{ref}^{node}(n, i_Y)$. To do this, we should transform the coordinates of these nodes from the reference local coordinate system to the actual local coordinate system taking into account actual aircraft position and orientation of the velocity vector. As a result, we obtain geometrically correct SAR looks on the rectangular grid (i_X, i_Y) on the ground plane.

The grid step in azimuth should be multiple of the reference pulse repetition path and should be small enough so that the nodes of the adjacent looks $x_{ref}^{node}(n, i_Y)$ and $x_{ref}^{node}(n+1, i_Y)$ do not coincide.

III. MULTI-LOOK RADIOMETRIC CORRECTION

The proposed SAR processing algorithm with built-in geometric correction works without clutter-lock. It means that some SAR look beams may be pointed at the ground areas which are not illuminated by the real antenna beam at the moment. In order to track the illuminated spot on the ground we propose to perform the multi-look SAR processing with an extended number of SAR looks so that the real antenna beam illuminates different SAR looks at different moments of time. It can be imaging as the SAR image "migrates" though different SAR looks.

We can use the Doppler centroid values estimated from the radar data to prevent the synthesis of those SAR look beams which are obviously beyond the real antenna beam. It allows us to reduce the computation burden. It is especially important when the variations of the antenna beam orientation are larger than the antenna beam width, and we have to increase the number of SAR looks considerably, although a few of the SAR looks are illuminated simultaneously.

In this section we show how to combine the SAR looks to obtain the multi-look SAR image without radiometric errors. Let us denote the error-free SAR image to be reconstructed as $I_0(x, y)$. The SAR looks can be written as

$$I(n; x, y) = I_0(x, y) \cdot N(n; x, y) \cdot R(n; x, y). \quad (11)$$

where $n = 1, ..., N_{LExt}$ is the look index, $N(n; x, y)$ represents multiplicative speckle noise, $0 < R(n; x, y) \le 1$ is the radiometric error function.

In order to estimate the brightness of SAR looks we should apply a two-dimensional low-pass filter $\mathbf{F}$ to suppress speckle noise. We shall assume that the filter preserves variations of

illumination (the radiometric errors) caused by the instabilities of the antenna beam orientation and removes most of the speckle noise:

$$\mathbf{F}\{R(n; x, y)\} \approx R(n; x, y), \quad \mathbf{F}\{N(n; x, y)\} \approx 1. \quad (12)$$

Under these assumptions, the application of the filter to the SAR looks gives approximately

$$\mathbf{F}\{I(n; x, y)\} = I_{LF}(n; x, y) \approx I_{0LF}(x, y)R(n; x, y). \quad (13)$$

Here $I_{0LF}(x, y)$ is the smoothed component of the SAR image to be reconstructed. The low-frequency image $I_{LF}(n; x, y)$ will be used to extract information about the radiometric errors.

The first step of the algorithm is to compose a sequence of "the best SAR looks". Each part of the scene is always presented in several SAR looks. We should select the brightest (best-illuminated) parts of the scene among all N_{LExt} extended SAR looks and use these parts to compose "the best SAR looks". The best SAR looks organized into a sequence of pairs $\{I_{Best}(n; x, y), I_{BestLF}(n; x, y)\}$, $n = 1, ..., N_{LBest}$ in the ascending order with respect to brightness $I_{BestLF}(n; x, y) < I_{BestLF}(n+1; x, y)$.

The sequence is composed as follows. We take the SAR look one-by-one (all of N_{LExt} looks) and smooth it by the low-pass filter. Then we compare the brightness of the obtained smoothed SAR look $I_{LF}(n; x, y)$ pixel-by-pixel with the already composed smoothed best SAR looks $I_{BestLF}(n; x, y)$ trying to insert the new pairs $\{I(n; x, y), I_{LF}(n; x, y)\}$ into the sequence preserving the ascending order.

The best SAR look with index N_{LBest} is composed of the brightest parts selected among all N_{LExt} SAR looks. According to the idea of the proposed radiometric correction procedure, this composed SAR look does not suffer from radiometric errors. For this look $R(N_{LBest}; x, y) \approx 1$ and, according to (13), we can use it as the reference to estimate the error-free low-frequency component of SAR image:

$$I_{0LF}^{Est}(x, y) \approx I_{BestLF}(N_{LBest}; x, y). \quad (14)$$

Now from (13) we can find the radiometric error functions for all of N_{LBest} looks as

$$R_{Best}^{Est}(n; x, y) \approx \frac{I_{BestLF}(n; x, y)}{I_{0LF}^{Est}(x, y)}. \quad (15)$$

The correction of radiometric errors is performed as

$$I_{Best}^{RC}(n; x, y) = I_{Best}(n; x, y)\frac{I_{0LF}^{Est}(x, y)}{I_{BestLF}(n; x, y)}. \quad (16)$$

Finally, these looks can be summed up into the multi-look SAR image with corrected radiometry.
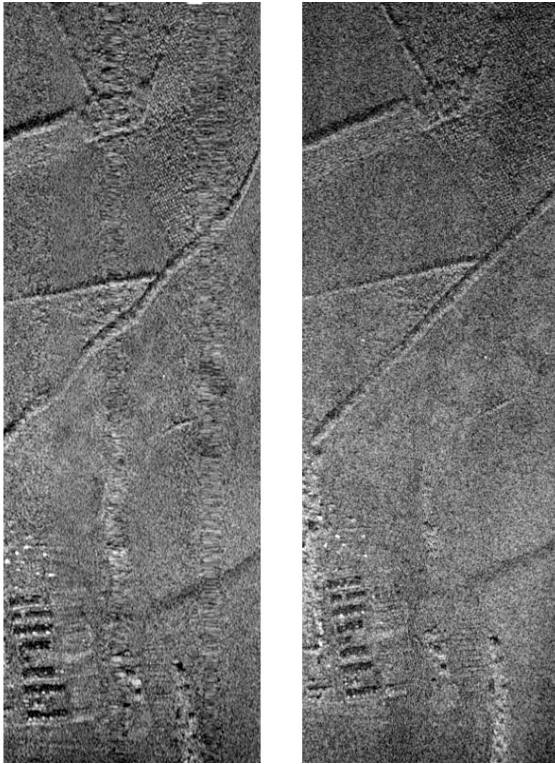
Fig. 2: The left SAR image is built by using clutter-lock. The right SAR image is formed by using the built-in geometric correction.

Fig. 3: SAR image (45 looks) formed by using the built-in geometric correction is imposed on the Google Map image.

IV. EXPERIMENTAL RESULTS

The proposed SAR processing algorithm has been tested with a Ku-band SAR system installed on a light-weight aircraft. The left SAR image in Fig. 2 was built by using clutter-lock. One can see significant geometric distortions caused by instabilities of the antenna orientation. The right SAR image in this figure is formed by using the algorithm with the built-in geometric correction. Both images have 3-m resolution and were built by using 3 looks.

The accuracy of the geometric correction is illustrated in Fig. 3 where the 45-look SAR image formed by using the built-in geometric correction is imposed on the Google Map image of the scene. One can see that the proposed algorithm allows us to obtain high-quality multi-look SAR images.

V. CONCLUSION

Pros of the proposed algorithms:

1. No additional interpolation of SAR images is required. SAR images are already geometrically correct after synthesis.

2. Reduced requirements to motion compensation. Trajectory deviations should be measured and compensated with the high accuracy of a fraction of the radar wavelength only during the time of synthesis of one look (0.25 s for 3-m resolution). In order to build the multi-look image, the trajectory should be measured with the accuracy of a fraction of the SAR resolution during the time of data acquisition for all looks (12.5 s for 99 looks).

3. Operation from light-weight aircraft and UAV platforms with a non-stabilized or fixed-mounted antenna.

4. Operation with a not very expensive navigation system. Orientation measurements are not required.

5. Producing multi-look images by using as many looks as possible with the real antenna beam width.

Cons of the proposed algorithms:

1. Lots of computations in case of SAR imaging with very high resolution because of the long time-domain convolution.

2. Other SAR processing methods are more efficient if the SAR system is equipped with a stabilized antenna and a good navigation system, and full motion compensation is performed.

REFERENCES

[1] C. J. Oliver, S. Quegan, *Understanding Synthetic Aperture Radar Images.* Boston; London: Artech House, 1998.

[2] S. Buckreuss, "Motion errors in an airborne synthetic aperture radar system", *European Transactions on Telecommunications*, Vol. 2, No. 6, pp. 655–664, 1991.

[3] D. Blacknell et al., "Geometric accuracy in airborne SAR images", *IEEE Trans. on Aerospace and Electronic Systems*, Vol. 25, No. 2, pp. 241-258, March 1989.

[4] S. N. Madsen, "Estimating the Doppler centroid of SAR data", *IEEE Trans. on Aerospace and Electronic Systems*, Vol. 25, No. 2, pp. 134-140, March 1989.

[5] D. M. Vavriv et al, "Cost-effective Ku-band airborne SAR with Doppler centroid estimation, autofocusing and indication of moving targets", *Proc. 2nd European Radar Conf. EuRAD2005*, Paris, France, pp. 21-24, 2005.

[6] A. Moreira, "Improved Multilook Techniques Applied to SAR and SCANSAR Imagery", *IEEE Trans. on Geoscience and Remote Sensing*, Vol. 29, No. 4, pp. 529-534, July 1991.

[7] O.O. Bezvesilniy, I.V. Dukhopelnykova, V.V. Vinogradov and D.M.Vavriv, "Retrieving 3-D topography by using a single-antenna squint-mode airborne SAR", *IEEE Trans. on Geoscience and Remote Sensing*, Vol. 45, No. 11, pp. 3574-3582, 2007.

[8] O.O. Bezvesilniy, V.V. Vinogradov and D.M.Vavriv, "High-Accuracy Doppler Measurements for Airborne SAR Applications", *Proceedings of the 5th European Radar Conference EuRAD2008*, Amsterdam, The Netherlands, pp. 29-32, 2008.